10.21611/qirt.2020.149

QIRT PORTO – PORTUGAL 2020, 6-10 JULY 15th Quantitative InfraRed Thermography Conference1

Latent Low Rank Representation Applied to Thermography

J. FLEURET[1,2], C. IBARRA-CASTANEDO[1,2], S. EBRAHIMI[1,2], X. MALDAGUE[1,2]

[1]Faculty of Sciences and Engineering, University Laval, Quebec City, Quebec, Canada, julien.fleuret.1@univ.laval.ca
[2]Laboratory of Computer Vision and Numerical Systems, Multipolar Infrared Vision team, Quebec City, Quebec, Canada

1 Abstract

This paper introduce a evaluate the Latent Low-Rank Representation (LatLRR) on pulsed thermographic data. The LatLRR decompose an image on a linear association of three kind of informations, observed, unobserved and noise. These information are then used in order to separate the salient and principal features. This study has found that when use as a post processing tool or when a state of the art method is apply on any features the LatLRR failed to provide any valuable results. Nevertheless the results when applied on the best image of a state of the art method allow a significant improvement regarding the detection of the defects.

Keywords— latLRR, Latent Low-Rank Representation, active thermography, material, defect detection, Pulst Thermography

2 Introduction

Infrared Non-Destructive Testing (IRNDT) is a field that uses thermal sources and appropriate sensors in order to evaluate samples of interest in order to assess their quality. A popular application of IRNDT is Pulsed Thermography (PT). In PT a very short pulse of energy is applied to a sample of interest. Often the pulse is realized using powerful flash lamps. When the pulse reaches the sample, the energy of the pulse is converted into heat and becomes a thermal front which will spread into the sample. The presence of voids, cracks, foreign material inserts, as well as local variation of density will create a local variation in the absorption of the energy, which will be acquired by a thermal camera. The popularity of PT comes from the simplicity of its implementation, its relative low-cost and it is able to work with a wide range of materials. However because thermal cameras are sensitive to a wide range of noises, Over the years several approaches have been proposed in order to improve the detection of defects. Maldague et al. [1] have proposed the Pulsed Phase Thermography (PPT). Based on the phase of the signal in a Fourier domain, this method is robust to many noise sources such as non-uniform heating, reflection and geometry. The defects of the contrast in the signal make them easier to find. Later Shepard et al. [2] proposed the Thermographic Signal Reconstruction (TSR). The TSR consists in modeling the behavior of the sample subjeted to a heat-pulse as a polynomial regression of the data into a natural logarithmic space. This approach significantly increases the robustness of the reconstructed signal. Shepard et al. [2] highlight that the first and second polynomial derivative of the signal allow the detection of defects even in very noisy data. TSR is robust to noise but is sensitive to over-illumination and non-uniform heating. It is often used as a preprocessing step in association with another approach. Rajic et al. [3] have studied the application of the Principal Component Analysis (PCA) to PT (under the name PCT) which became very well-known for its simplicty, the quality of the results it provides as well as dimensional reduction it offers. It is sensitive to over-illumination and non-uniform heating; other types of noises also affect the results but not significatively. More recently Lopez et al. [4, 5] have proposed an approach in order to both reconstruct and detect defects by apply a Partial Least Squares regresson the acquisition. The Partial Least Squares Thermography (PLST) provides comparable results with those obtained with the PCT with a significant lower Signal over Noise Ratio (SNR). However the PLST is sensitive to gradient inversion. Over the years, improvement of these works as well as new approaches have been proposed [6–11]. This study focuses on the application of Latent Low-Rank Representation (LatLRR) [12], which express any signal as the linear relashion of three type of informations, observed, unobserved and noise. The separations between each representation are expressed as an optimization of a low-rank convex problem. The next section intoduces the LatLRR from a more theoretical point of view. The application of LatLRR to the processing of data acquired during PT is detailed in section 4. Section 5 describes the experiment and details the methodology regarding the study. The results are introduced in section 6 and discussed in section 7. Section 8 concludes this study.

10.21611/qirt.2020.149

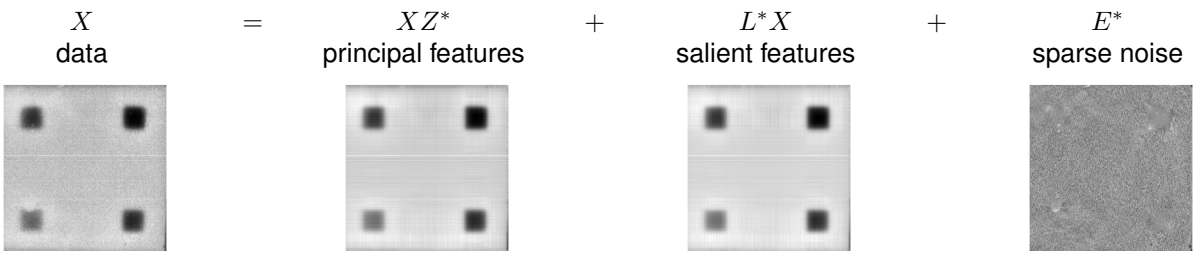

Figure 1

3 Latent Low Rank Representation

The Latent Low Rank Representation has been introduced by Liu et al. [12] as an improvement of the existing Low Rank Representation (LRR). The goal of each approach concerns robust subspace segmentation. In the LRR approach the data is considered a set of representation vectors structurate as a dictionary. The aim of LRR is to find the lowest rank representation among the candidates that is the most suitable to fit the data.

$$\underset{Z}{min}\|Z\|_*\,,\ s.t.\ X_O = AZ \tag{1}$$

In (1) the variable X_O represents the matrix of observations, each column is an observation vector and the whole matrix is composed of *k* subspaces $\{\mathbf{S}_{i=1}^k\}$ and each one has a rank denoted r_i. X_O can be expressed as the collection of n_i samples from each subspace $X_O = [X_1, X_2, \cdots, X_k]$ and is sufficient if and only if for every rank $X_i = r_i, \forall i$. A represents the dictionary and $\|.\|_*$ represents the nuclear norm, i.e. the sum of the singular values of the matrix. A common practice to solve this equation for subspace segmentation applications consists in setting the observed data as a dictionary. The optimization problem in that case become:

$$\underset{Z}{min}\|Z\|_*\,,\ s.t.\ X_O = X_O Z \tag{2}$$

In a perfect case when the data is noiseless and the number of samples sufficient, solving (2) may work. However often either the data are corrupted by noise or the number of samples is insufficient, if it is not both. If the input dictionary does not have sufficient samples, then equation (2) will not converge. A lack of samples in the input dictionary means that equation (2) will converge to an identity matrix. The noise in the data will significantly influence the accuracy of the subspace clustering. In an attempt to increase the robustness to noise another formulation has been proposed.

$$\underset{Z}{min}\|Z\|_*\,,\ s.t.\ X_O = [X_O, X_H]Z \tag{3}$$

Like for equation (1) the term X_O still designates the matrix of observations, the new term X_H designate the unobserved hidden data. The addition of X_H in the cost function makes it robust to insufficient data sampling. Nevertheless Liu et al. [12] have shown that the formulation in equation (3) is ill-posed because the optimal solution is computed which updates X_O and X_H is computed from them without any constraints.
The LatLRR is a reformulation of the LRR which introduces two regulatization terms in order to properly model both the noise as well as the unobserved informations.

$$\underset{Z,E}{min}\|Z\|_* + \lambda\|E\|_1\,,\ s.t.\ X_O = [X_O, X_H]Z + E \tag{4}$$

In equation (4) $\|.\|_1$ designates the norm ℓ_1 and E represents the sparse noise.
Liu et al. [12] have demonstrate extensively the robustness of the LatLRR for the cases of noisy data and corrupted data. The appliction of the LatLRR to thermography enables the ability to enhance the data and reduce the noise without requiring any prior.

4 LatLRR applications to NDT

To the best of the knowledge of the authors there was no previous application of the LatLRR to thermography, which offers a wide range of possibilities. The ability of the LatLRR to represent the content of an image as

10.21611/qirt.2020.149

the linear combinaison of three matrices, one representing the salient information, one representing the hidden unobserved data and at last one representing the noise, which offers many possibilities of investigations. This study investigates four possible applications. The first application is the ability of the LatLRRT to improve the result obtained from the application of state of the art approaches on a dataset. This experiment aim to improve the quality of a detection by reconstructing it with only some of the signals it is composed of e.g. reconstructing the signal only with the principal and salient features. The improvement that can be offered by removing the sparse noise of a sequence before applying a detection algorithm is then investigated. After applying the LatLRR on a sequence, each features matrix as well as the noise are stored separately before a detection algorithm is applied on each sequence. This aims to investigate the possibility of improving the detections of existing algorithms by analysing separately the features of the images of a sequence. At last the possibility to use the LatLRR as a detection algorithm is investigated. For this investigation due to the computationality of LatLRR the data used are subsampled from the data acquired during the experiments.

5 Method

The goal of this study is to evaluate and assess the interest of LatLRR to improve the detection of defects in materials. To do so, we conducted experiments on a reference sample of Carbon Fiber Reinforced Plastic (CFRP) that contains twenty-five Teflon inserts. These defects are divided into five batches of five defects. Each batch has five inserts having the same depth but different sizes (from 3x3 mm^2 to 15x15 mm^2). Also, as illustated in figure 2, each batch has been positioned at a specific depth (from 0.2 to 1 mm). The materials have

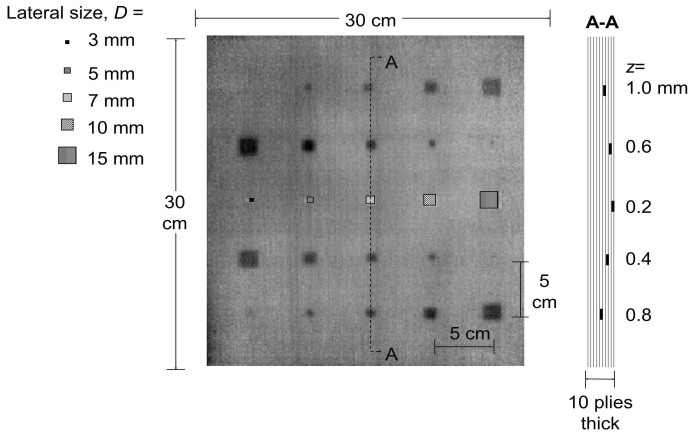

Figure 2: CFRP sample used for the experiments.

been investigated by a classic pulse thermographic procedure. Each material has been stimulated from the front side by a pulse generated by two photographic flashes (Balcar FX 60, $5\ ms$ thermal pulse, $6.4\ kJ/flash$). A mid-wave infrared (MWIR) camera FLIR Phoenix ($1.5\ \mu m$ to $5.0\ \mu m$, $345\ Hz$, 14 bit per pixel, 640×512) was used for data acquisition. For each experiment, a sequence of the 2000 frames was acquired during a period of 30 seconds. That duration ensured that both the warm-up and the cool-down period had been acquired by the sensor.

Once the raw data was acquired three test sets are generated. The first processing consists computing the cold image, shrinking the datasets in order to only keep the data that has been acquired after the pulse, and subtracting the cold image. Pulsed Phase Thermograpy (PPT) [1] and Principal Component Thermography (PCT) [3] algorithms have processed the each dataset. In our experiments we chose $N = 400$.

In order to assess the interest of the proposed approach, it was compared with the state of the art and one metrics has been selected. The proposed approach has four possible interests. It is able to separate the noise and generate a representation for both observed and unobserved data from an input signal. This allows an investigation of the improvement that the noise removal offers when associated with state of the art processing as well as the influence of each signal on the final result. Due to the computational cost of this approach,

10.21611/qirt.2020.149

it should be investigated in two steps. Another experiment of interest is the use of the proposed approach to improve the result of the state of art methods. First the LatLRR is applied on each image separately, while during the second time a reduced dataset is processed as a whole. In order to assess the quality of each experiment we chose to use the Signal over Noise Ratio (SNR). We useds the formulation proposed by Usamentiaga et al. [13]

$$SNR(roi_s, roi_n) = \frac{|\mu_s - \mu_n|}{\sqrt{\frac{(\sigma_s^2 + \sigma_n^2)}{2}}} \tag{5}$$

6 Results

As visible in figure 3, the application of the LatLRR on each image separately before the application of PCT failed to provide any valuable results. The same conclusion has been made when the PPT is applied on the same context. For this reason the SNR has not been computed for this experiment. Figures 5 shows the evolution of the mean of the SNR values regarding both the depth and the size of the defects. Figure 4 shows the different features, the sparse noise as well as a noiseless reconstruction of the data. This reconstruction is made using only the principal and salient features. The table 1 computes the SNR values of all the defects of the reference. For the situation where a image sequence is sent as a whole to be processed by the LatLRR, no results have been generated. This experiment has failed to give any valuable results.

7 Discussion

As visible in figure 3 when state of the art methods are applied on every dataset indenpendently as well as the noiseless reconstructed dataset, they fail to provide significant results. However this highlighs that the computation of the salient features try to reconstruct the information per column while the principal features try to reconstruct the information per rows. The experiments conducted on the best images selected from the results of the PCT and PPT provide surprising results. One can note from figure 4 that not only is LatLRR able to capture the information in the image as well as the sparse noise, but one can notice on the PPT results that it can significantly improve the results. The best image resulting from the application of the PPT on the sample shows some defects but suffers from an extremly low contrast. Both principal and salient features are able to capture the information and to enhance the contrast, making the defects significantly easier to detect. From figure 5 one can note that the SNR values of the sparse noise (E) are very low and vary in a very small range which means that sparse noise images do not contains any information that could lead to the detection of defects. From the processing of the best image resulting from the PCT, the SNR values of the principal and salient features follow the same trend in terms of variations regarding both the size of the defect as well as its depth, as the one computed from the best image (X). Note that salient and principal features have a higher range of values than the one computed from the best image, which shows that they have a better contrast. The results computed from the best image resulting from the PPT, show that the salient and principal features SNR's values follow two different trends. These different trend can be observed regarding both the size of the defects and their depth. From figure 4 it is visible that for the PPT data, both salient and principal features offer a better contrast than the best image. However the SNR values shows that the salient features are lower than the SNR of the input data, which usually means that the quality of the image would be lower than that input image. From a visual point of view it is not the case. This likely means that because of the optimization, the standard deviation of both the sound area and the defect are significantly higher than in the best image. The means are also higher but as visible in (5) the magnitude of the standard deviation between the defect and the sound area will have a greater influence on the results. Principal features always have higher SNR value which means that it has a better contrast than the image it has been computed from. Neverhteless from a visual point of view principal features often offer a smoother image. To conclude this experiment one can observe that for both PPT and PCT best images the reconstructed image based on salient and principal features offers a better image than the one given as input. The experiment conducted consisted to use the LatLRR on a whole dataset have failed, for this reason no results have been generated. When used after resizing the input image to a size of 128 x 128 pixels it has failed to converge after 12 hours of computation. The 12 hour duration was chosen arbitrarily, however most state of the art approaches are able to provide results within minutes. If the experiment would have provided a results within two hours with the same quality as the one observed in figure 4 the method could have been suitable as an offline post processing approach. Another trial was after

10.21611/qirt.2020.149

		Depth (mm) \ Lateral size (mm)	3	5	7	10	15
PCT	X	0.2	1.6859	0.975	0.3801	1.5951	0.6465
		0.4	0.6631	1.2896	0.929	1.1817	1.3934
		0.6	1.4082	1.0591	0.2326	1.5675	0.6902
		0.8	1.6177	1.9137	0.4004	1.6049	0.4785
		1.0	0.3956	1.458	0.1188	2.2263	2.0732
	PF	0.2	1.92	0.9917	0.3591	2.2248	0.9109
		0.4	0.8958	1.8074	0.7518	1.1554	1.1953
		0.6	1.1271	1.1834	0.2498	1.9306	0.7141
		0.8	2.0827	3.3014	0.4111	1.5971	0.5972
		1.0	0.2594	1.7139	0.1079	3.0746	2.4539
	SF	0.2	2.0034	0.9321	0.327	2.2148	0.8996
		0.4	0.9098	1.8145	0.8079	1.1086	1.2883
		0.6	1.1066	1.1596	0.2195	1.9302	0.7554
		0.8	2.0943	3.4038	0.3607	1.5813	0.7454
		1.0	0.3629	1.7143	0.0568	3.1769	2.4716
	E	0.2	0.0	0.0	0.1057	0.016	0.0675
		0.4	0.0426	0.1117	0.1705	0.0	0.0
		0.6	0.0	0.1127	0.1044	0.0325	0.0461
		0.8	0.1237	0.1265	0.1379	0.1695	0.0
		1.0	0.0279	0.2188	0.0601	0.0602	0.2239
	R	0.2	1.9653	0.9652	0.3439	2.221	0.9063
		0.4	0.903	1.8113	0.7805	1.135	1.244
		0.6	1.118	1.1733	0.2354	1.9309	0.734
		0.8	2.0903	3.35	0.3871	1.5908	0.6702
		1.0	0.3102	1.7149	0.0834	3.1226	2.4645
PPT	X	0.2	1.1694	0.0165	1.4056	2.1804	0.4962
		0.4	0.9602	2.6609	3.6683	1.0726	1.8115
		0.6	0.3436	1.7565	4.8142	4.51	1.3995
		0.8	1.4626	1.4584	2.0114	0.844	1.8016
		1.0	0.7055	1.4804	2.2744	3.7462	2.4145
	PF	0.2	2.4125	1.4218	2.7483	3.6607	0.803
		0.4	1.2385	3.3436	4.0681	2.4953	1.2078
		0.6	0.2657	2.7596	4.6401	4.7838	1.7253
		0.8	1.7717	3.0717	2.7756	1.6297	1.7186
		1.0	0.7772	2.3789	2.2824	4.433	2.6864
	SF	0.2	2.2479	0.6655	1.4645	0.8296	0.7596
		0.4	0.8333	1.1712	1.4313	0.7076	2.5681
		0.6	1.3322	0.7389	1.6442	1.2568	0.4588
		0.8	1.5944	1.8158	2.3842	0.8854	2.5182
		1.0	2.767	0.6957	1.8379	2.0015	1.8733
	E	0.2	0.1219	0.1527	0.1159	0.0336	0.0426
		0.4	0.0068	0.1063	0.0723	0.104	0.0627
		0.6	0.1269	0.0767	0.202	0.0264	0.1104
		0.8	0.077	0.1043	0.1538	0.0525	0.0278
		1.0	0.1158	0.1074	0.0645	0.0621	0.165
	R	0.2	3.3412	1.0991	2.5278	2.8347	0.7963
		0.4	1.0807	2.9202	3.684	1.7731	2.3807
		0.6	0.2173	1.8976	3.912	3.931	1.2058
		0.8	1.7151	2.9037	2.8361	1.2952	2.9322
		1.0	1.9543	1.5984	2.2287	3.8583	2.3776

Table 1: SNR computed on the best image resulting from the processing of PCT and PPT methods (X), the Principal Features (PF), the Salient Features (SF), the sparse noise (E), and the reconstructed image R

10.21611/qirt.2020.149

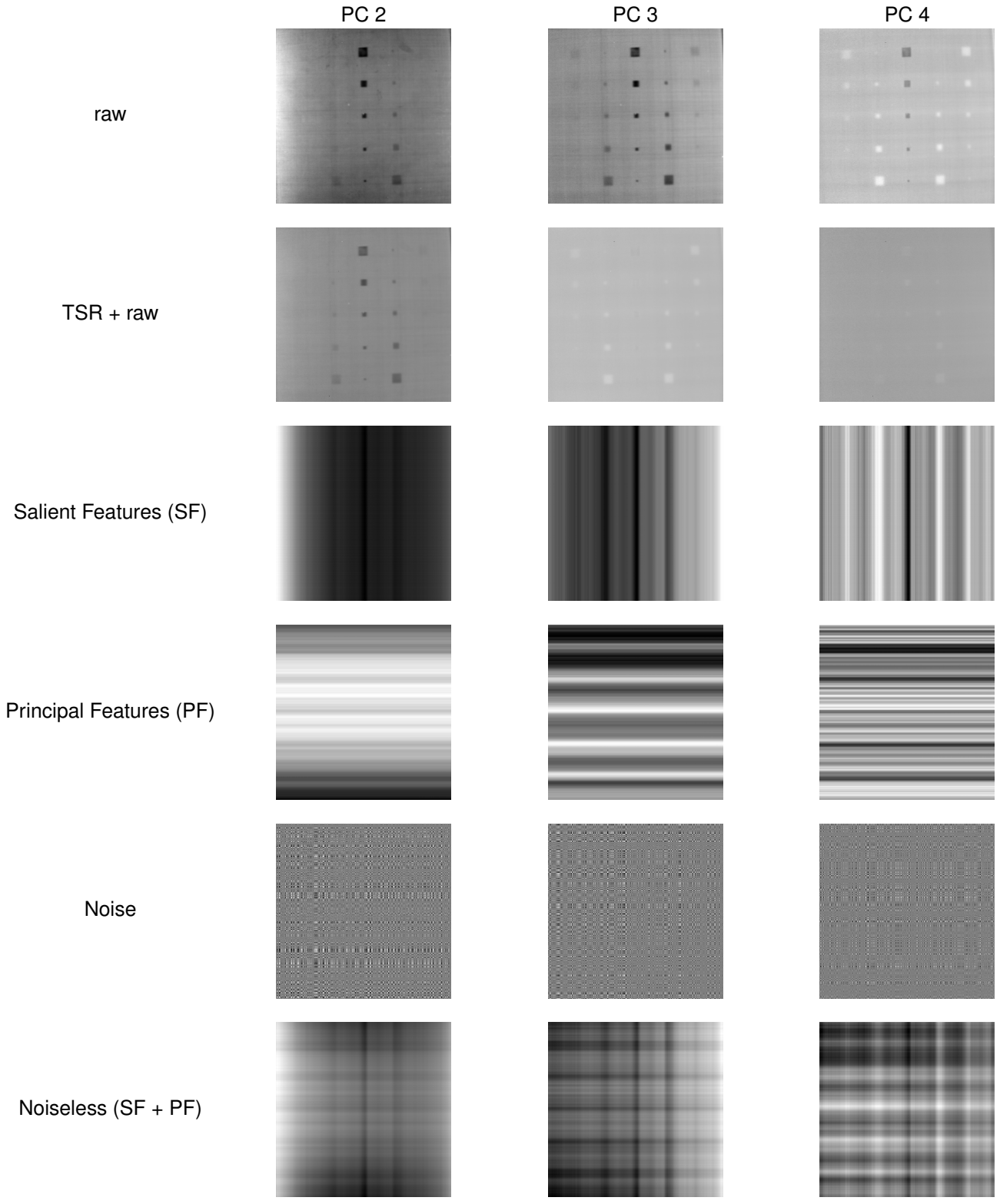

Figure 3: Results of the best principal components after application of the PCT.

reducing the size of the images to a size of 32 x 32 pixels. It has converged within a few minutes but has entirely failed to capture any information. Reducing the size of the image using interpolation approaches changes the information on the image. Depending on the scale of the reduction some information such as edges may be

10.21611/qirt.2020.149

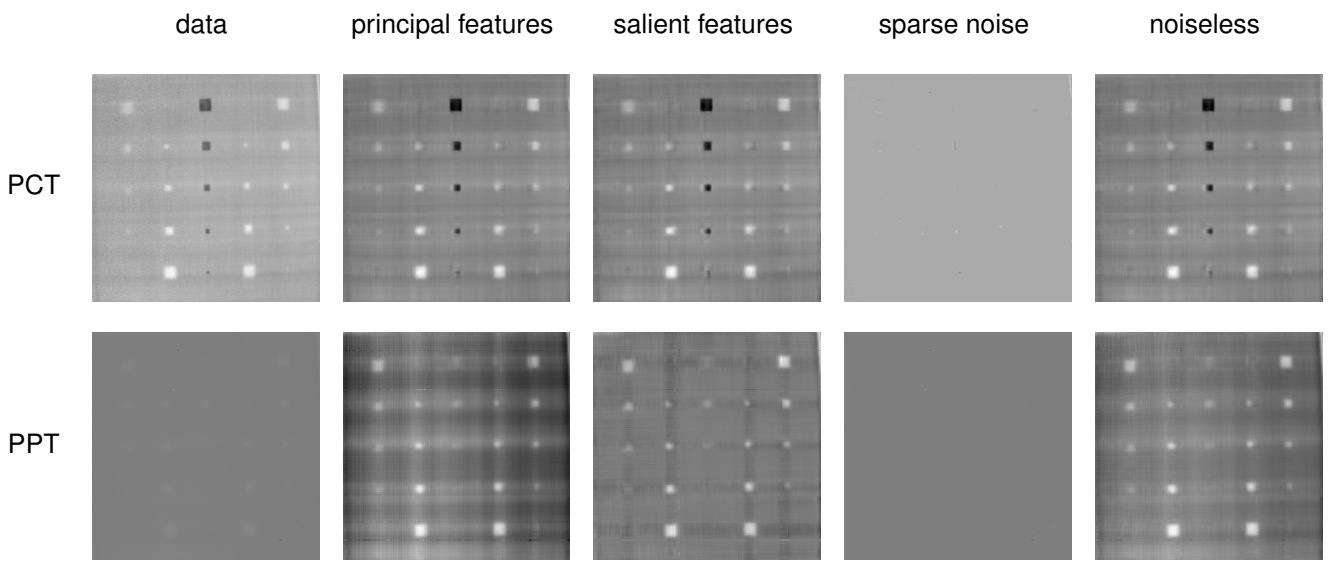

Figure 4: Visualization of the different signals regarding the improvement of the best images selected from the results of state of the art approaches.

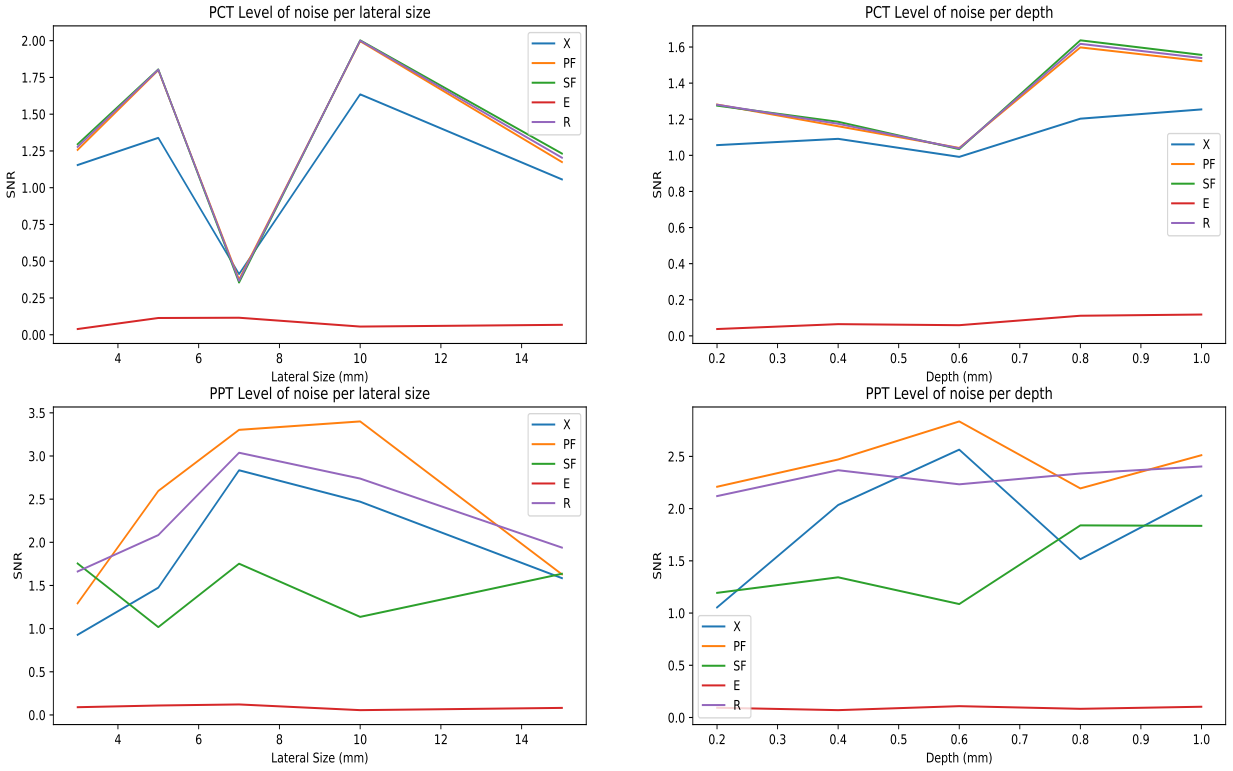

Figure 5: Evolution of the mean SNR regarding the depth and lateral size for PCT and PPT and for each signal.

less affected than other like the texture, nevertheless if the reduction is to low most of the informations are lost. It is likely to be the reason of the failure of the last experiment when used on the image of size 32 x 32 pixels. This study shows that the LatLRR is a great tool in order to improve the results of state of the art method in

10.21611/qirt.2020.149

a acceptable computation time (within minutes). More works are needed in order to investigate its interest on different materials.

8 Conclusion

This paper studied the potential application of the Latent Low-Rank Representation (LatLRR) to IRNDT. Four experiments have been conducted in order to evaluate the interest of this method on image sequences acquired using pulsed thermography. Applying LatLRR on the image sequence before apply state of the art method on either the features, the sparse noise a reconstructed image based on the summation of the features failed to give any valuable results. Apply LatLRR on the results of a state of the art on the best image resulting of a state of the art approach give good results even when the best image has a poor contrast. The application of the LatLRR on a whole has failed to provide any results, nevertheless the main reason of this failure is related to the computational cost . In this study the LatLRR has show its ability to be a greatly improve the results of state of the art approaches, in a relatively acceptable computation time (within few minutes).

Acknowledgement

This research was supported by the Fonds Quebecois de Recherche - Nature et Technologie (FQRNT).
The authors would like to thank Annette Schwerdtfeger for the time and energy she spent reviewing this article.

References

[1] Xavier Maldague and Sergio Marinetti. Pulse phase infrared thermography. *Journal of applied physics*, 79(5):2694–2698, 1996.

[2] Steven M Shepard. Advances in pulsed thermography. In *Thermosense XXIII*, volume 4360, pages 511–515. International Society for Optics and Photonics, 2001.

[3] Nikolas Rajic. Principal component thermography. Technical report, DEFENCE SCIENCE AND TECHNOLOGY ORGANISATION VICTORIA (AUSTRALIA . . . , 2002.

[4] Fernando Lopez, Vicente Nicolau, Xavier Maldague, and Clemente Ibarra-Castanedo. Multivariate infrared signal processing by partial least-squares thermography. In *ISEM Conference*, 2013.

[5] Fernando Lopez, Clemente Ibarra-Castanedo, Vicente de Paulo Nicolau, and Xavier Maldague. Optimization of pulsed thermography inspection by partial least-squares regression. *Ndt & E International*, 66:128–138, 2014.

[6] Bardia Yousefi, Stefano Sfarra, Clemente Ibarra Castanedo, and Xavier PV Maldague. Thermal ndt applying candid covariance-free incremental principal component thermography (ccipct). In *Thermosense: Thermal Infrared Applications XXXIX*, volume 10214, page 102141I. International Society for Optics and Photonics, 2017.

[7] Bardia Yousefi, Hossein Memarzadeh Sharifipour, Clemente Ibarra Castanedo, and Xavier PV Maldague. Automatic irndt inspection applying sparse pca-based clustering. In *2017 IEEE 30th Canadian Conference on Electrical and Computer Engineering (CCECE)*, pages 1–4. IEEE, 2017.

[8] Bardia Yousefi, Stefano Sfarra, Fabrizio Sarasini, and Xavier PV Maldague. Irndt inspection via sparse principal component thermography. In *2018 IEEE Canadian Conference on Electrical & Computer Engineering (CCECE)*, pages 1–4. IEEE, 2018.

[9] Bardia Yousefi, Stefano Sfarra, Fabrizio Sarasini, Clemente Ibarra Castanedo, and Xavier PV Maldague. Low-rank sparse principal component thermography (sparse-pct): Comparative assessment on detection of subsurface defects. *Infrared Physics & Technology*, 98:278–284, 2019.

[10] Sergio Marinetti, Ermanno Grinzato, Paolo G Bison, Edoardo Bozzi, Massimo Chimenti, Gabriele Pieri, and Ovidio Salvetti. Statistical analysis of ir thermographic sequences by pca. *Infrared Physics & Technology*, 46(1-2):85–91, 2004.

10.21611/qirt.2020.149

[11] J Fleuret, C Ibarra-Castanedo, L Lei, S Sfarra, R Usamentiaga, and X Maldague. Defect detection based on monogenic signal processing. In *Algorithms, Technologies, and Applications for Multispectral and Hyperspectral Imagery XXV*, volume 10986, page 109861X. International Society for Optics and Photonics, 2019.

[12] Guangcan Liu and Shuicheng Yan. Latent low-rank representation for subspace segmentation and feature extraction. In *2011 International Conference on Computer Vision*, pages 1615–1622. IEEE, 2011.

[13] R Usamentiaga, Clemente Ibarra-Castanedo, and X Maldague. More than fifty shades of grey: Quantitative characterization of defects and interpretation using snr and cnr. *Journal of Nondestructive Evaluation*, 37(2):25, 2018.